ACS APPLIED ENERGY MATERIALS

www.acsaem.org

Letter

Multinuclear Solid-State NMR Study of the Aqueous Solid-Electrolyte Interphase Formation in $NaTi_2(PO_4)_3$

Vytautas Klimavičius,* Nadežda Traškina, Aurimas Dubauskas, Matas Manionis, Jurgis Pilipavičius, and Linas Vilčiauskas*

Cite This: *ACS Appl. Energy Mater.* 2024, 7, 11665−11669

Read Online

ACCESS | Metrics & More | Article Recommendations | Supporting Information

ABSTRACT: Solid-electrolyte interphases enable stable operation of non-aqueous Li-ion batteries, but their formation, especially in aqueous systems, is not well understood. NASICON-structured $NaTi_2(PO_4)_3$ is a widely studied ion insertion negative electrode material for various aqueous electrochemical applications. This study uses multinuclear ^{31}P, ^{23}Na, ^{13}C, $^{47,49}Ti$ solid-state NMR to examine $NaTi_2(PO_4)_3$ aqueous degradation and solid-electrolyte interphase formation. The results indicate that interphase consists of amorphous phases similar to $TiO(OH)(H_2PO_4)\cdot nH_2O$ and carboxylic groups on carbonaceous phases, formed through electrochemical degradation. The formation of the aqueous solid-electrolyte interphase results in low Coulombic efficiency, pronounced self-discharge, and capacity loss of $NaTi_2(PO_4)_3$ during charge−discharge cycling.

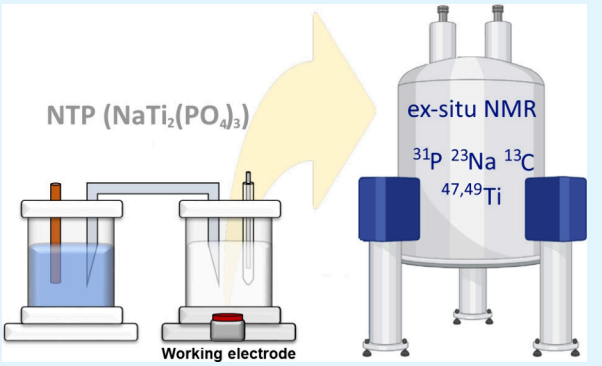

KEYWORDS: *NASICON, NTP, aqueous batteries, solid-state NMR, ex situ*

The ongoing transition to renewable energy and sustainable materials ecosystems requires new technological developments such as electrochemical energy devices.[1,2] This is due to their (i) high operational efficiencies, (ii) high selectivity, and (iii) flexible size/power scaling. For example, lithium-ion batteries achieved remarkable economies of scale and enabled new applications ranging from portable electronics to personal mobility. However, several issues related to materials criticality, environmental footprint, and system safety remain. Therefore, there is an intense search and development of various alternative technologies based on noncritical electrode materials, simple and safe aqueous electrolytes, and novel cell concepts.[3,4] Solid-electrolyte interphase is one of the key features enabling the stable operation of conventional nonaqueous Li-ion batteries. Although these interphases are intensively researched, the detailed structure and dynamics is still far from being completely understood. Even less is known about these layers and their properties in aqueous systems.

$NaTi_2(PO_4)_3$ (NTP) having NASICON structure is one of the most studied and widely applied ion insertion negative electrode materials for aqueous electrochemical devices such as batteries and Faradaic deionization cells.[5−11] This is due to its (i) favorable electrode potential of the $Ti^{(III)}/Ti^{(IV)}$ redox couple (−0.62 V vs standard hydrogen electrode (SHE)) close to the hydrogen evolution reaction, (ii) relatively high specific charge capacity (133 mAh g^{-1}) for a two-electron redox process, and (iii) robust open framework structure facilitating high ion mobility. However, under typical operating conditions, NTP-based electrodes show relatively low Coulombic efficiency (CE), pronounced self-discharge, and capacity loss during charge−discharge cycling.[6−8,12] Hydrogen evolution (HER) and oxygen reduction (ORR) reactions are deemed to be the main parasitic processes competing with Na-ion de/insertion. HER which is more pronounced in acidic electrolytes reduces the CE and leads to local alkalization. Electrochemical ORR involving the reduction of O_2 dissolved in electrolyte on the electrode surface also leads to lower CE and local alkalization. Finally, a chemical ORR which is a reaction between $Ti^{(III)}$ generated in the charge state of NTP and dissolved O_2 results in self-discharge which lowers the CE and causes local alkalization.[6−8] Our previous study showed that NTP capacity loss is negligible until pH ∼ 7 but becomes pronounced already at pH ∼ 8. This confirms that the local electrolyte alkalization is the main cause of NTP degradation and electrochemical activity loss.[6−8] However, *post mortem* powder X-ray diffraction phase analysis, and energy dispersive X-ray spectroscopy determined element ratios showed that only ∼20% of the observed capacity loss can be directly related to the degradation of the NTP phase itself.[8] Therefore, the

Received: August 30, 2024
Revised: December 2, 2024
Accepted: December 2, 2024
Published: December 5, 2024

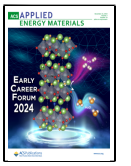

NTP electrochemical activity loss in aqueous electrolytes was attributed to the formation of interphasial layers which block Na-ion and/or electron transport.[6−8] Such layers until now were deemed to be composed of NTP aqueous degradation products such as amorphous $Ti(H_2PO_4)_x(HPO_4)_{2-x/2} \cdot nH_2O$ phases.[6−8]

A detailed understanding of the degradation processes and aqueous solid-electrolyte interphase formation is essential for developing novel degradation prevention and mitigation strategies and enabling NTP applications in practical electrochemical devices. Unfortunately, many widely used analytical techniques such as X-ray diffraction are not suitable due to the amorphous nature of such interphasial layers. Therefore, such methods as solid-state Nuclear Magnetic Resonance (ssNMR) spectroscopy can provide invaluable insights. In this study, we use multinuclear ^{31}P, ^{23}Na, $^{47,49}Ti$, and ^{13}C *ex situ* ssNMR spectroscopy of NTP-based electrodes to analyze their degradation in aqueous electrolytes during electrochemical cycling. The obtained results clarify some important questions and misconceptions regarding the degradation products and processes in NTP during its aqueous electrochemical operation.

The detailed preparation protocol of NTP electrodes is given in Supporting Information. NTP electrodes were galvanostatically charge−discharge (GCD) cycled in naturally aerated 1 M Na_2SO_4(aq.) solutions under flooded electrolyte conditions to induce NTP degradation and facilitate the ssNMR analysis. The capacity retention results in Figure 1

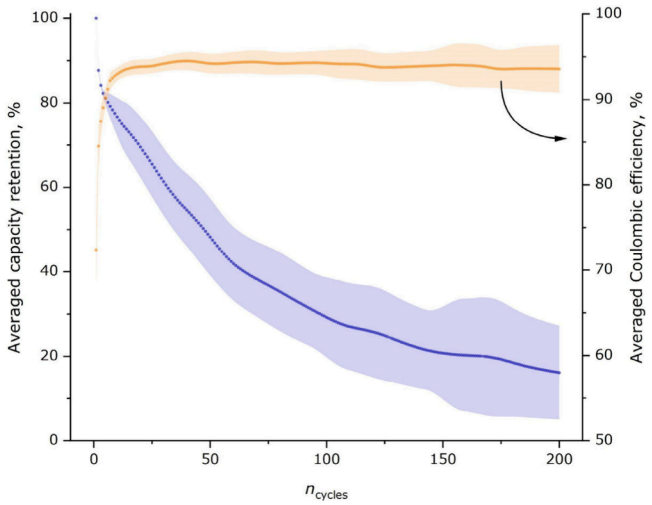

Figure 1. Averaged relative discharge capacity retention of NTP electrodes during GCD cycling in naturally aerated 1 M Na_2SO_4(aq.).

show that NTP electrodes, on average, lose ∼60% and ∼80% of their initial capacity within 100 and 200 GCD cycles, respectively. At these conditions, the electrolyte typically reaches pH ∼ 10 due to parasitic HER and ORR reactions, even with some buffering provided by dissolving CO_2 which could readily react with OH^-.[8] Therefore, most of the observed NTP capacity loss is usually attributed to the degradation caused by electrolyte alkalization. The NTP electrode samples were cycled for 0, 50, 100, 150, and 200 predefined full charge−discharge cycles and taken out of the cell for *ex situ* ssNMR analysis (see Supporting Information for details).

The evolution of phosphorus species during electrochemical NTP cycling was analyzed by ^{31}P magic-angle spinning (MAS) ssNMR. The complete set of data using various relaxation filters together with the NMR spectral library of relevant phosphate phases are presented in Supporting Information. The representative spectra obtained using a 1 s relaxation filter show a sharp line at −27.9 ppm corresponding to the NTP phase (Figure 2a).[13] However, another much broader feature centered around ∼2 ppm with FWHM = 2.8 kHz emerges during cycling. Because there are no other characteristic features in the ^{31}P MAS ssNMR spectra, this broad line is attributed to the NTP degradation products. The position of the line at ∼2 ppm strongly suggests that most of the phosphorus must be in $H_2PO_4^-$ form likely coordinated by aqueous-like species (H_2O, OH^-, O^{2-}). On the other hand, it also implies that most of the titanium should also be more likely coordinated by aqua, hydroxyl, and oxyl rather than phosphate groups. Therefore, we suggest that amorphous phases observed at ∼2 ppm have a composition similar to the previously reported $TiO(OH)(H_2PO_4)\cdot nH_2O$ (−7 ppm)[14,15] with some remaining surface or trapped H_3PO_4/$H2PO_4^-$ rather than commonly suggested $Ti(HPO_4)_2\cdot H_2O$ (−18 ppm).[14−18] The evolution of this phase during cycling was analyzed by evaluating the spectral line integral ratio between the line attributed to amorphous species and that of the total NMR spectrum (I_{amorph}/I_{total}). The results in Figure 2b show the amorphous phase starting to form immediately after NTP comes into contact with aqueous electrolyte. Interestingly, it grows in the first 100 GCD cycles but then begins to fade. This suggests that amorphous titanium phosphates are likely forming blocking interphasial layers during cycling which are responsible for most of the electrochemical activity loss in NTP. However, under flooded electrolyte conditions the degradation products might also dissolve back into the electrolyte as indicated by the fade of a ^{31}P MAS ssNMR spectral line. The strong presence of phosphates in the electrolyte after cycling was also confirmed by our previous ICP-OES results.[7]

The degradation of NTP was also analyzed by ^{23}Na MAS ssNMR. The spectra presented in Figure 3 obtained using 10 s relaxation delay show the main spectral feature corresponding to NTP (δ_{iso} = −14.5 ppm, C_Q = 2.9 MHz, η = 0) which is in agreement with previously reported values.[13] The traces of $Na_2SO_4 \bullet nH_2O$ left over in a porous electrode after washing are visible at 0.1 ppm in some samples.[25−27] However, there is another broader feature appearing at −11.5 ppm indicating the formation of additional sodium-containing phases during NTP cycling. Interestingly, this feature is visible even in the fully relaxed ^{23}Na MAS spectra (relaxation delay >5T_1 see Figure 3 and Figures S7−S12 in Supporting Information). In order to further investigate ^{23}Na data, ^{23}Na MQMAS spectrum was obtained which shows two highly overlapped lines at around −11.5 ppm and the third much broader and less intense line which is partly overlapped with the NTP signal (Figures 3b and S13). This indicates three inequivalent Na sites in the amorphous phase. Very similar features were previously reported for NaOH-activated porous carbons and attributed to the sodium ions bonded to the oxygenated surface functional groups at the edge of graphene planes.[19] In this study, we also attribute the feature at −11.5 ppm to sodium ions bound to surface-carboxylate groups.[20−22] For further analysis the spectral lines are approximated with a single line having both Gaussian and Lorentzian contributions (Figure

https://doi.org/10.1021/acsaem.4c02224
ACS Appl. Energy Mater. 2024, 7, 11665−11669

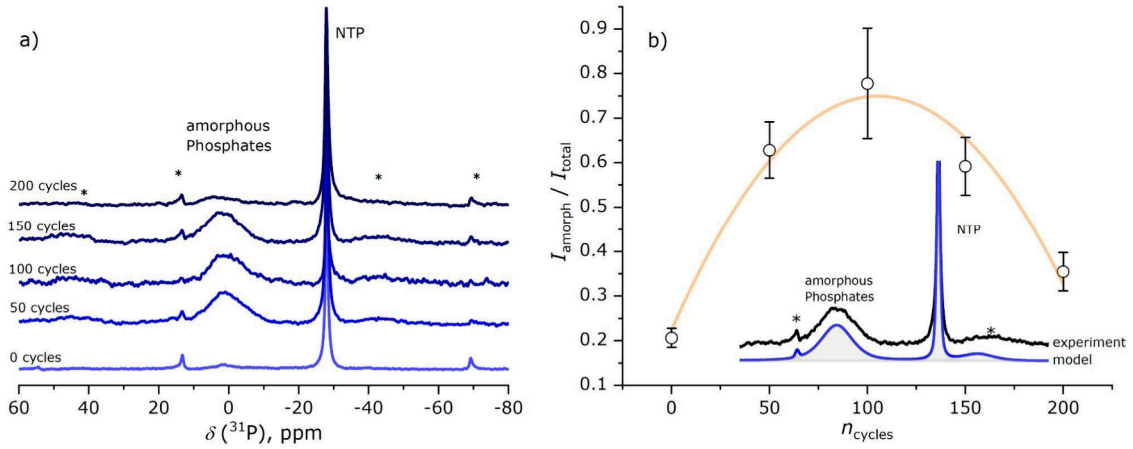

Figure 2. a) *ex situ* ^{31}P MAS ssNMR spectra of NTP electrodes and b) evolution of the I_{amorph}/I_{total} integral ratio during GCD cycling. Asterisks indicate MAS spinning sidebands; 1 s relaxation filter was used. The error bars originate from the spectral fitting.

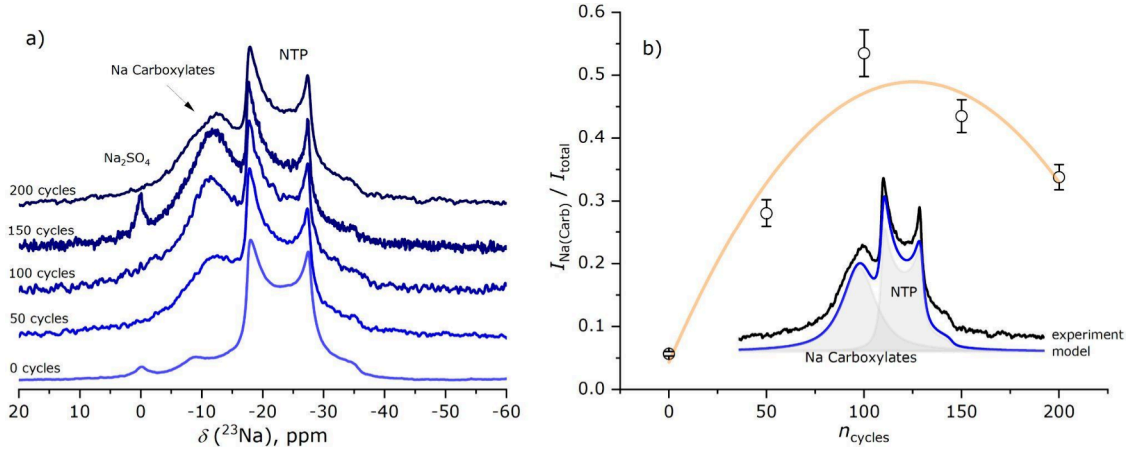

Figure 3. a) *ex situ* ^{23}Na MAS ssNMR spectra of NTP electrodes with relaxation delay of 10 s (fully relaxed) and b) evolution of the $I_{Na(Carb)}$ /I_{total} integral ratio during GCD cycling. Error bars originate from the spectral fitting.

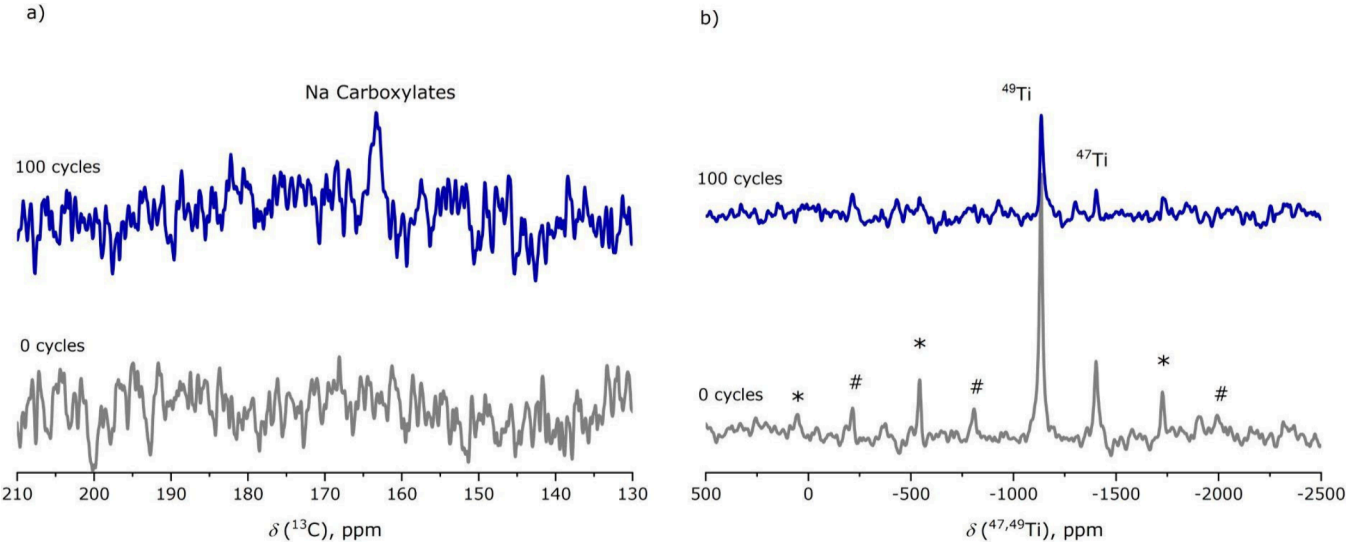

Figure 4. *Ex situ* a) ^{13}C CP MAS (130−210 ppm region) and b) ^{47,49}Ti MAS ssNMR spectra of NTP electrodes before (gray) and after 100 GCD cycles (blue). Asterisks and hashtags indicate ^{47}Ti and ^{49}Ti MAS spinning sidebands, respectively.

3b). In order to study the dynamical evolution of Na species during cycling, the spectral line integral ratio between the Na-carboxylate line and that of the total NMR spectrum ($I_{Na(Carb)}$-/I_{total}) is introduced (Figure 3b). Similarly to the ^{31}P results (Figure 2b), the ratio $I_{Na(Carb)}/I_{total}$ also increases up to 100 GCD cycles and decreases afterward. As discussed

https://doi.org/10.1021/acsaem.4c02224
ACS Appl. Energy Mater. 2024, 7, 11665−11669

previously, the likely explanation is due to two competing processes: the formation of surface Na-carboxylate species upon cycling and their dissolution into electrolyte once most of the NTP electrochemical activity is lost. The results suggest that the formation of surface carboxylate groups must be a much faster and efficient process than the formation of the amorphous phosphate species during cycling because it is visible in the ssNMR spectra without using ^{23}Na relaxation filters.

The formation of surface Na-carboxylates is also corroborated by ^{13}C CP MAS ssNMR experiments. The ^{13}C CP MAS spectra presented in Figure 4a show a line at 163 ppm which only appears after 100 GCD cycles but is absent in uncycled NTP. This feature is also attributed to the degradation of the porous carbon which is oxidized to form carboxylic groups on the surface edges during electrode degradation.[23,24] The obtained ^{31}Na and ^{13}C ssNMR results strongly suggest that there is some degradation of the carbonaceous phase in typical composite electrodes during electrochemical cycling in aqueous electrolytes. This degradation also contributes to the capacity loss since it reduces the contact of NTP particles with the electronically conducting carbon phase.

Although ^{47,49}Ti MAS ssNMR is less widely used for studying Ti-containing battery materials, it is an effective probe for detecting slight changes in the electronic structure of titanium species.[28,29] To the best of our knowledge, the ^{47,49}Ti NMR spectrum of pure NTP has not been reported before. Titanium occupies a highly symmetric site (Wyckoff position 12c) in the NPT structure, therefore the ^{47,49}Ti MAS NMR spectrum consists of two spectral lines at −1402 ppm and −1133 ppm attributed to ^{47}Ti and ^{49}Ti resonances, respectively (Figure S14 in Supporting Information). The spectrum does not feature dominant quadrupolar line shape broadening due to a highly symmetric Ti environment even though ^{47}Ti is I = 5/2 and ^{49}Ti is I = 7/2.

^{47,49}Ti MAS NMR spectra of NTP electrodes before and after GCD cycling are shown in Figure 4b. The ^{47,49}Ti MAS NMR electrode spectra feature the resonances at the same chemical shift as pure NTP. Although a visible loss of signal intensity is detected after 100 GCD cycles, we refrain from quantitative assumptions due to high signal-to-noise ratio. Nevertheless, ^{47,49}Ti MAS NMR data indicate no detectable amounts of Ti-containing degradation products such as $TiO(OH)(H_2PO_4)\cdot nH_2O$. It is important to note that due to quadrupolar broadening, previous ^{47,49}Ti ssNMR data for crystalline $TiO(OH)(H_2PO_4)\cdot H_2O$ also show features that are difficult to assign.[15] Therefore, in the case of amorphous phases similar to $TiO(OH)(H_2PO_4)\cdot nH_2O$, the ^{47,49}Ti spectrum should feature extremely broad featureless lines that are masked within the background signal.

In this study, a multinuclear ^{31}P, ^{23}Na, ^{13}C and ^{47,49}Ti, *ex situ* solid-state NMR spectroscopy is used to study the degradation of $NaTi_2(PO_4)_3$ electrodes during electrochemical cycling in naturally aerated aqueous 1 M Na_2SO_4 electrolytes. The electrode samples were cycled for 0, 50, 100, 150, and 200 full charge−discharge cycles, respectively, and taken out of the cell for the *ex situ* NMR investigation. The results suggest that (i) the formation of amorphous phases with a composition similar to $TiO(OH)(H_2PO_4)\cdot nH_2O$ are more likely than commonly suggested $Ti(HPO_4)_2\cdot H_2O$, (ii) these phases form blocking layers which reduce the electrochemical activity of $NaTi_2(PO_4)_3$, (iii) oxidation of carbon surface to carboxylic groups also contributes to capacity loss, (iv) two competing processes are taking place during galvanostatic charge−discharge cycling i.e. formation and growth of amorphous phase which is dominating in the beginning and their dissolution into the electrolyte once $NaTi_2(PO_4)_3$ electrochemical activity is lost. Finally, the potential and versatility of ^{47,49}Ti ssNMR for studying Ti-based materials is demonstrated.

■ ASSOCIATED CONTENT

Supporting Information

The Supporting Information is available free of charge at https://pubs.acs.org/doi/10.1021/acsaem.4c02224.

Experimental details and additional NMR data (PDF)

■ AUTHOR INFORMATION

Corresponding Authors

Vytautas Klimavičius − *Institute of Chemical Physics, Vilnius University, LT-10257 Vilnius, Lithuania*; Email: vytautas.klimavicius@ff.vu.lt

Linas Vilčiauskas − *Center for Physical Sciences and Technology (FTMC), LT-10257 Vilnius, Lithuania; Institute of Chemistry, Vilnius University, LT-10257 Vilnius, Lithuania*; orcid.org/0000-0002-1256-9777; Email: linas.vilciauskas@ftmc.lt

Authors

Nadežda Traškina − *Center for Physical Sciences and Technology (FTMC), LT-10257 Vilnius, Lithuania*

Aurimas Dubauskas − *Institute of Chemical Physics, Vilnius University, LT-10257 Vilnius, Lithuania*; orcid.org/0009-0009-4398-9377

Matas Manionis − *Institute of Chemical Physics, Vilnius University, LT-10257 Vilnius, Lithuania*

Jurgis Pilipavičius − *Center for Physical Sciences and Technology (FTMC), LT-10257 Vilnius, Lithuania; Institute of Chemistry, Vilnius University, LT-10257 Vilnius, Lithuania*

Complete contact information is available at: https://pubs.acs.org/10.1021/acsaem.4c02224

Author Contributions

V.K.: funding acquisition, project administration, resources, conceptualization, methodology, supervision, investigation, formal analysis, data curation, visualization, validation, writing-original draft, writing-review and editing. N.T.: methodology, investigation, formal analysis, data curation, visualization, validation, writing-original draft. A.D.: methodology, investigation, formal analysis, data curation, visualization, validation, writing-original draft. M.M.: methodology, investigation, formal analysis, data curation, visualization, validation, writing-original draft. J.P.: conceptualization, methodology, investigation, supervision, formal analysis, data curation, visualization, validation, writing-original draft. L.V.: resources, conceptualization, methodology, supervision, investigation, formal analysis, data curation, visualization, validation, writing-original draft, writing-review and editing. The manuscript was written through the contributions of all authors. All authors have approved the final version of the manuscript.

Notes

The authors declare no competing financial interest.

https://doi.org/10.1021/acsaem.4c02224
ACS Appl. Energy Mater. 2024, 7, 11665−11669

■ ACKNOWLEDGMENTS

This project has received funding under the grant agreement with the Research Council of Lithuania (LMTLT) (Project No. S-MIP-23-47). V.K., A.D., and M.M. acknowledge the Center of Spectroscopic Characterization of Materials and Electronic/Molecular Processes (SPECTROVERSUM Infrastructure) for the use of NMR spectrometers.

■ REFERENCES

(1) Gallo, A. B.; Simões-Moreira, J. R.; Costa, H. K. M.; Santos, M. M.; Moutinho dos Santos, E. Energy Storage in the Energy Transition Context: A Technology Review. *Renew. Sustain. Energy Rev.* **2016**, *65*, 800−822.
(2) Stamenkovic, V. R.; Strmcnik, D.; Lopes, P. P.; Markovic, N. M. Energy and Fuels from Electrochemical Interfaces. *Nat. Mater.* **2017**, *16*, 57−69.
(3) Chao, D.; Zhou, W.; Xie, F.; Ye, C.; Li, H.; Jaroniec, M.; Qiao, S.-Z. Roadmap for Advanced Aqueous Batteries: From Design of Materials to Applications. *Sci. Adv.* **2020**, *6*, No. eaba4098.
(4) Wu, D.; Li, X.; Liu, X.; Yi, J.; Acevedo-Peña, P.; Reguera, E.; Zhu, K.; Bin, D.; Melzack, N.; Wills, R. G. A.; Huang, J.; Wang, X.; Lin, X.; Yu, D.; Ma, J. 2022 Roadmap on Aqueous Batteries. *J. Phys. Energy* **2022**, *4*, No. 041501.
(5) Park, S. I.; Gocheva, I.; Okada, S.; Yamaki, J.-I. Electrochemical Properties of $NaTi_2(PO_4)_3$ Anode for Rechargeable Aqueous Sodium-Ion Batteries. *J. Electrochem. Soc.* **2011**, *158*, A1067.
(6) Mohamed, A. I.; Whitacre, J. F. Capacity Fade of $NaTi_2(PO_4)_3$ in Aqueous Electrolyte Solutions: Relating pH Increases to Long Term Stability. *Electrochim. Acta* **2017**, *235*, 730−739.
(7) Pleckaityte, G.; Petruleviciene, M.; Staisiunas, L.; Tediashvili, D.; Pilipavicius, J.; Juodkazyte, J.; Vilciauskas, L. Understanding and Mitigation of $NaTi_2(PO_4)_3$ Degradation in Aqueous Na-Ion Batteries. *J. Mater. Chem. A* **2021**, *9*, 12670−12683.
(8) Pilipavičius, J.; Traškina, N.; Juodkazytė, J.; Vilčiauskas, L. The Mechanism of $NaTi_2(PO_4)_3$ Aqueous Electrochemical Degradation Revisited. *Electrochim. Acta* **2023**, *465*, No. 142993.
(9) Liu, X.; Xu, X.; Xuan, X.; Xia, W.; Feng, G.; Zhang, S.; Wu, Z.-G.; Zhong, B.; Guo, X.; Xie, K.; Yamauchi, Y. Unlocking Enhanced Capacitive Deionization of $NaTi_2(PO_4)_3$/Carbon Materials by the Yolk-Shell Design. *J. Am. Chem. Soc.* **2023**, *145*, 9242−9253.
(10) Delmas, C.; Cherkaoui, F.; Nadiri, A.; Hagenmuller, P. A NASICON-Type Phase as Intercalation Electrode: $NaTi_2(PO_4)_3$. *Mater. Res. Bull.* **1987**, *22*, 631−639.
(11) Santos, C.; La Mantia, F. Insights into Desalination Battery Concepts: Current Challenges and Future Perspectives. *Chem. Commun.* **2023**, *59*, 6437−6452.
(12) Zhan, X.; Shirpour, M. Evolution of Solid/aqueous Interface in Aqueous Sodium-Ion Batteries. *Chem. Commun.* **2017**, *53*, 204−207.
(13) Bradtmüller, H.; Nieto-Muñoz, A. M.; Ortiz-Mosquera, J. F.; Rodrigues, A. C. M.; Eckert, H. Glass-to-Crystal Transition in the NASICON Glass-Ceramic System $Na_{1+x}Al_xM_{2-x}(PO_4)_3$ (M = Ge, Ti). *J. Non Cryst. Solids* **2018**, *489*, 91−101.
(14) Li, Y.; Whittingham, M. Hydrothermal Synthesis of New Metastable Phases: Preparation and Intercalation of a New Layered Titanium Phosphate. *Solid State Ionics* **1993**, *63*−*65*, 391−395.
(15) Rusanova-Naydenova, D.; Trublet, M.; Klysubun, W.; Cholsuk, C.; Iuga, D.; Dupree, R.; Antzutkin, O. N.; Persson, I. Synthesis and structural characterisation of solid titanium(IV) phosphate materials by means of X-ray absorption and NMR Spectroscopy. *Dalton Trans.* **2022**, *51*, 8192−8207.
(16) Schmutz, C.; Barboux, P.; Ribot, F.; Taulelle, F.; Verdaguer, M.; Fernandez-Lorenzo, C. EXAFS, Raman and ^{31}P NMR Study of Amorphous Titanium Phosphates. *J. Non Cryst. Solids* **1994**, *170*, 250−262.
(17) Trublet, M.; Maslova, M. V.; Rusanova, D.; Anzutkin, O. N. Mild syntheses and surface characterization of amorphous $TiO(OH)(H_2PO_4)\cdot H_2O$ ion-exchanger. *Mater. Chem. Phys.* **2016**, *183*, 467−475.
(18) Maslova, M.; Ivanenko, V.; Gerasimova, L.; Larsson, A.-C.; Antzutkin, O. N. Synthesis of titanium Phosphates from unconventional solid precursor and their ion-exchange and electrochemical properties. *J. Mater. Sci.* **2021**, *56*, 9929−9950.
(19) Freitas, J. C. C.; Schettino, M. A., Jr; Emmerich, F. G.; Wong, A.; Smith, M. E. A multiple-field ^{23}Na NMR study of sodium species in porous carbons. *Solid State Nucl. Magn. Reson.* **2007**, *32*, 109−117.
(20) Xu, M.; Harris, K. D. M. Triple-Quantum ^{23}Na MAS NMR Spectroscopy as a Technique for Probing Polymorphism in Sodium Salts. *Cryst. Growth Des.* **2008**, *8*, 6−10.
(21) Dusek, M.; Chapuis, G.; Meyer, M.; Petricek, V. Sodium Carbonate Revisited. *Acta Crystallogr. B* **2003**, *59*, 337−352.
(22) Reeve, Z. E. M.; Franko, C. J.; Harris, K. J.; Yadegari, H.; Sun, X.; Goward, G. R. Detection of Electrochemical Reaction Products from the Sodium−Oxygen Cell with Solid-State ^{23} Na NMR Spectroscopy. *J. Am. Chem. Soc.* **2017**, *139*, 595−598.
(23) Klimavicius, V.; Neumann, S.; Kunz, S.; Gutmann, T.; Buntkowsky, G. Room temperature CO oxidation catalysed by Supported Pt nanoparticles revealed by solid-state NMR and DNP Spectroscopy. *Catal. Sci. Technol.* **2019**, *9*, 3743−3752.
(24) Nebel, H.; Neumann, M.; Mayer, C.; Epple, M. On the Structure of Amorphous Calcium Carbonate—A Detailed Study by Solid-State NMR Spectroscopy. *Inorg. Chem.* **2008**, *47*, 7874−7879.
(25) Borchardt, L.; Oschatz, M.; Paasch, S.; Kaskel, S.; Brunner, E. Interaction of electrolyte molecules with carbon materials of well-defined porosity: characterization by solid-state NMR Spectroscopy. *Phys. Chem. Chem. Phys.* **2013**, *15*, 15177−15184.
(26) Lyu, D.; Märker, K.; Zhou, Y.; Zhao, E. W.; Gunnarsdóttir, A. B.; Niblett, S. P.; Forse, A. C.; Grey, C. P. Understanding Sorption of Aqueous Electrolytes in Porous Carbon by NMR Spectroscopy. *J. Am. Chem. Soc.* **2024**, *146*, 9897−9910.
(27) Luo, Z.-X.; Xing, Y.-Z.; Ling, Y.-C.; Kleinhammes, A.; Wu, Y. Electroneutrality breakdown and specific ion effects in nanoconfined aqueous Electrolytes Observed by NMR. *Nat. Commun.* **2015**, *6*, 6358.
(28) Lätsch, L.; Kaul, C. J.; Yakimov, A. V.; Müller, I. B.; Hassan, A.; Perrone, B.; Aghazada, S.; Berkson, Z. J.; De Baerdemaeker, T.; Parvulescu, A.-N.; Seidel, K.; Teles, J. H.; Copéret, C. NMR Signatures and Electronic Structure of Ti Sites in Titanosilicate-1 from Solid-State $^{47/49}Ti$ NMR Spectroscopy. *J. Am. Chem. Soc.* **2023**, *145*, 15018−15023.
(29) Lucier, B. E. G.; Huang, Y. Reviewing $^{47/49}Ti$ Solid-State NMR Spectroscopy: From Alloys and Simple Compounds to Catalysts and Porous Materials. *Annu. Rep. NMR Spectrosc.* **2016**, *88*, 1−78.

https://doi.org/10.1021/acsaem.4c02224
ACS Appl. Energy Mater. 2024, 7, 11665−11669